Reliability assessment of land subsidence monitoring results using PSI technique in Ho Chi Minh City, Vietnam

Vu Thi Phuong Thao, Dang Truong Giang & Le Vu Anh

Published online: 07 Mar 2024.

Submit your article to this journal ⬀

View related articles ⬀

View Crossmark data ⬀

Routledge
Taylor & Francis Group

Check for updates

ARTICLE

Reliability assessment of land subsidence monitoring results using PSI technique in Ho Chi Minh City, Vietnam

Vu Thi Phuong Thao[a], Dang Truong Giang[b] and Le Vu Anh[c]

[a]Department of Environment Engineering, Hanoi University of Mining and Geology, Ministry of Education and Training of Vietnam, Hanoi, Vietnam; [b]National Remote Sensing Department, Ministry of Natural Resources and Environment of Vietnam, Hanoi, Vietnam; [c]Department of Mathematics and Computer Science, Beloit College, Beloit, WI, USA

ABSTRACT

Groundwater exploitation, soft ground, and urban development are the main causes of land subsidence in Vietnam. This study focuses on identifying, zoning, monitoring, and evaluating land subsidence using PSI technique with IBI method applied to Ho Chi Minh City. The results show diverse land subsidence trends from 2014 to 2021 with different levels in varying locations 98,278 km^2 had subsided by over 10 cm, 214,593 km^2 had subsided by 5 to 10 cm, and 1.377,897 km^2 had subsided by less than 5 cm. Notably, certain areas have higher subsidence funnel centres. To ensure accuracy when using PSI techniques, both natural and human-induced factors must be considered during data collection, which influences the actual subsidence rate. Though difficult, this technique provides reliable insights into this complex phenomenon, e.g. in the geodetic precise levelling method to detect millimetre-level deformations in urban areas. The average PS density in urban areas is between 0,5% and 2,5% of the original number of pixels. The positioning accuracy of a PS is within 1 m in all three directions if a large number of SAR scenes are used. Therefore, the results have been documented with 1 mm precision.

Introduction

Land subsidence is an important problem in major urban areas of Vietnam, such as Hanoi, Ho Chi Minh City, and the Mekong Delta region. There are serious efforts to investigate the causes and propose solutions to mitigate and rectify ground subsidence phenomena. Ground subsidence has undergone extensive study and research in Vietnam over time.

Vietnam has unique geographical features. There is a long coastline, 3,260 km long. There are 2,360 rivers with a length greater than 10 km on a small strip of land, 331.690 km^2. There is a tropical monsoon climate. Many storms are prolonged and of high intensity. These natural factors partly cause land subsidence. In addition, resource exploitation activities, especially groundwater exploitation, land use conversion activities,

CONTACT Vu Thi Phuong Thao ✉ vuthiphuongthao@humg.edu.vn; vtpthao1975@gmail.com ⬚ Department of Environment Engineering, Hanoi University of Mining and Geology, Ministry of Education and Training of Vietnam, 18 Duc Thang, Bac Tu Liem, Hanoi 10053, Vietnam

and economic activities change soil composition, geological structure and ecological conditions have contributed to increasing land subsidence [1].

Land subsidence needs to be mapped to plan and structure the city and so that appropriate actions may be taken to anticipate and map the impacts. Land subsidence can be determined by Multi-temporal Synthetic Aperture Radar (SAR) Interferometry (InSAR). The application of satellite radar data provides the ability to detect and monitor ground deformation with centimetre-to-millimetre, offering greater spatial detail and the capability to cover remote areas [2].

Sandwell and Price assumed that the atmospheric phase is a random process in time and that displacement exhibits a linear trend [3]. They proposed the stacking InSAR algorithm. Ferretti et al. [4] and Ferretti et al. [5] found that when the amplitude deviation of a pixel is within a specific range, the pixel's phase stability is better [4,5]. They named these pixels 'permanent scatterers' (PSs). When the time-series cumulative phase of these PSs is retrieved from the single master stack interferograms, this method is referred to as permanent scatterer interferometry (PSI): which has been significantly refined to detect and quantify land subsidence over wide areas. The PSI technique shows two main limitations: (1) the PSI measurements represent the cumulative ground movements, which can complicate the interpretation of ground deformation processes; (2) most of the geological processes are non-linear, with seasonal and multi-year components that are difficult to identify only through the average rate of displacements [6]. The PSI approach has demonstrated its capability in mapping ground deformation on a large spatial scale. With short-term data sampling rates based on the maximum likelihood estimator, it offers a rigorous way to exploit not only stable point-like scatterers PSs but also distributed scatterers (DS) [7].

Based on previous research results, Rosi et al. mentioned that PSI technique has proven to be highly valuable in measuring ground deformation associated with various geohazards such as landslides and subsidence [8]. In particular, the application of the PSI technique for subsidence mapping and characterisation provides the opportunity to detect this natural hazard with high precision (with a few metres of spatial resolution on the ground) and at a cost/measurement density not achievable with other field monitoring techniques. Furthermore, subsidence mapping using PSI technique benefits from the frequent occurrence of this phenomenon in urban areas, where a high density of PSs can be expected, ensuring high accuracy in measurements. Urban areas typically develop in plains, where ground deformation can be presumed vertical, making misinterpretation of movements unlikely. In addition, numerous applications of PSI for subsidence monitoring and simulation are documented in many publications [6,7,9–16].

Research by Holzer [17] and Ha et al. [18] indicates that severe problems caused by land subsidence have been observed in megacities worldwide, such as Bangkok (Thailand), Houston (USA), Mexico City (Mexico), Tokyo (Japan), Shanghai (China), and Venice (Italy) [17,18]. Over-extraction of groundwater, leading to a lowered water table, was identified as the primary cause of land subsidence in these cities [19]. Similarly, Nguyen [20] confirmed that groundwater exploitation is a primary contributor to land subsidence in Ho Chi Minh city, Vietnam.

Apart from groundwater-related causes of land subsidence in Ho Chi Minh City, Nguyen [20] highlighted that weak soil and rapid urbanisation are additional contributors to this phenomenon. Specifically, the terrain of Ho Chi Minh City represents a young

earth system that is gradually rising in elevation. The city is encircled by a network of canals and rivers. The geological structure of Ho Chi Minh City is characterised by weak soil and a high groundwater table. This foundation, coupled with construction activities, results in land subsidence. As construction density increases, so does the rate of subsidence.

This article focuses on some key issues: (1) assessing subsidence in Ho Chi Minh City using the PSI technique applied to the Sentinel-1 radar database for the period from 2014 to 2021; (2) enhancing the accuracy of results derived from the PSI technique by incorporating a filtering method that uses multi-temporal optical images; and (3) evaluating reliability through comparisons with field survey results obtained using the digital level machine during the same research period and by referencing published research findings [21–24].

Study area and data

Study area

Ho Chi Minh City, the study area, is one of five municipalities (centrally governed cities) in Vietnam. Spanning approximately 2095,239 km^2, it is situated between the coordinates
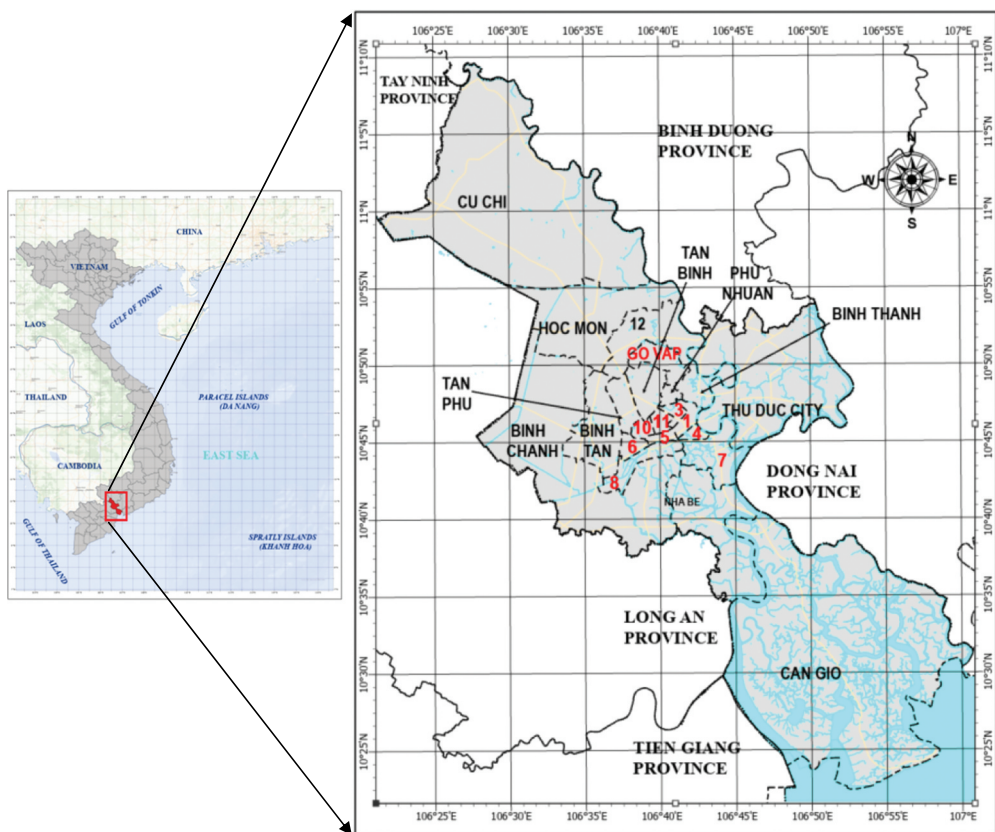

Figure 1. Map of Ho Chi Minh City in Vietnam.

10°10'–10°38' North and 106°22'–106°54' East (Figure 1). From an administrative stand-point, the city has 18 districts, one city, and five additional districts. Located in the Southeast region, Ho Chi Minh City is 50 km from the East Coast and lies in the transitional zone between the Southeast and the Mekong Delta. The city's topography descends from the North to the South and from West to East. The higher terrains are mainly in the North – Northeast and part of the Northwest, with altitudes ranging from 10 to 25 metres. There are a few hillocks, the tallest reaching up to 32 metres. Conversely, the lowlands are in the south-southwest and southeast of the city, with an average elevation of about 1 metre and the lowest point at 0,5 metres (HCM, 1). If one accounts for the rapid influx of undocumented individuals, population estimates approach 10 million inhabitants. This makes Ho Chi Minh City a megacity, as defined by the UN. Moreover, spatial trends in housing intensify the challenges tied to population growth. The built-up area of Ho Chi Minh City increased by 48,418 hectares between 1999 and 2015. Both the rate of urban expansion and suburbanisation are on the rise [14].

Data collection

Sentinel-1A remote sensing data of SLC (Single Look Complex) at level 1 was used to analyse land subsidence in Ho Chi Minh City using PSI technique. The Sentinel-1A data, consisting of 31 images, were collected between 2014 and 2021. The Interferometric Wide (IW) swath mode was the chosen beam mode, with area data paths and frames being 18 and 556, respectively. Data were gathered four times each year in February, March, November, and December. The year 2014 was an exception, as the IW format data covering the Ho Chi Minh City area only began on 23 November 2014. The choice of these specific months was strategic, aiming to avoid the rainy season. This minimises atmospheric influences on interference calculations owing to time differences over extended periods. Sentinel-1A constellations have a 12-day repeat cycle. The onboard C-band (~5.4 GHz) SAR sensor of Sentinal-1A captures high-resolution images in four standard operational modes: Strip Map (SM), Interferometric Wide swath (IW), Extra Wide swath (EW), and Wave (WV) modes [14]. Sentinel-1A data is freely accessible from various sources. In this study, data were sourced from the Alaska Satellite Facility's open data portal, chosen for its automated baseline assessment functionality. The Sentinel-1A Terrain Observation with Progressive Scan acquisition mode, combined with short temporal baselines, enhances the likelihood of coherent phase information between the master and slave images. This contributes to a potential increase in the density of PSs, beneficial for estimating deformation across a time series [14].

Results from a field survey monitoring land subsidence in Ho Chi Minh City from 2014–2020 of Dinh H.T.M [13] were compared to findings from a study using PSI based on Sentinel-1 data for 2017–2019 [14]. This comparison aimed to evaluate the reliability of the PSI technique for subsidence monitoring in this study.

Materials and methods

Holley et al. [9] noted that the results using PSI technique reveal diverse subsidence patterns across the city at different spatial scales. In certain areas, subsidence zones appear to be delineated by distinct lineaments. Some of these seem to correspond with

surface features, possibly indicating differences in land use or regions of industrial water abstraction. Yet, in other regions, there is no evident correlation with surface attributes. Such lineaments might be linked to deeper structural or tectonic factors. The basic steps employed in the study are as follows:

Data processing with PSI technique

The procedure for processing the Sentinel-1A imagery is detailed in the following steps. A crucial step in this phase is the creation of an image network. In this network, each slave image establishes a connection with its corresponding master image, as outlined in the network structure [4,25,26].

The next stage is informetric processing, which consists of several smaller steps: interferogram generation, phase flattening, and coherence estimation. All images are aligned with the master image and resampled with a coefficient of 4, mainly in the range direction. It is noteworthy that the selected PSI technique emphasises specific ground point objects to enhance accuracy. The master image acts as the foundational reference when generating interferograms for the slave images. To mitigate the effects of terrain errors, a Digital Elevation Model (DEM) is employed during the phase flattening stage. This ensures the extraction of accurate deformation values (relative to a particular ground reference point) by evaluating and subtracting errors contributed from atmospheric factors, orbital variations, and DEM itself [11]. Coherence estimation is integral to this process. The coefficient of variation (CoV) is particularly important in the analysis. It is calculated as $Ð = \mu/\sigma$, where μ is the temporal standard deviation of amplitude values, and σ signifies the temporal average amplitude value for each pixel. This metric allows for the identification of potentially coherent points without the need for an exhaustive phase value analysis. Since phase values at this stage still contain undetermined noise signals, the CoV metric offers an efficient way to pinpoint areas of coherent interest pragmatically [27].

The inverse displacement model, as outlined by Gaber et al. [28] is used to compute both the displacement velocity and the estimated residual height of the image point to the digital terrain model. To streamline the data, redundant phase values within the interferograms are eliminated based on the coherence index. This ensures that the subsequent processing considers only phase values that are reliable, stable, and correctly oriented. Furthermore, a linear model is used to derive and standardise the displacement velocity and residual height. A notable part of this process is filtering out oscillations in signal propagation delay. These oscillations mainly arise because of the influence of the tropospheric layer. To account for atmospheric effects and enhance the data's accuracy, both Low Pass and Hi Pass filtering techniques are incorporated. This methodology ensures that the displacement results for each specified time frame, as well as the reliable vertical subsidence velocity, are presented with high reliability and accuracy.

Finally, the conversion of displacement results for each specific timeframe and the vertical subsidence velocity in the previously mentioned 'range' direction is pivotal for deducing vertical subsidence values. By using the correlation values of each pixel, points with a high degree of correlation are selectively filtered and transformed from a raster format to a vector format. This transformation delivers PS points, enriched with details such as correlation, subsidence velocity, and

displacement for every individual time instance in the vertical axis. Subsequently, these refined results are channelled into data analysis, facilitating the creation of detailed subsidence progression maps and the construction of an exhaustive database.

Deformation data standardization

The IBI method cited by Chen et al. [11], Xu et al. [29] and Shan et al. [30] was used to depict land cover data, which were then integrated with land subsidence values obtained via the PSI technique to analyse their relationship. The IBI effectively minimises redundancy in multi-spectral images, reducing spectral confusion among land cover types. Consequently, it suppresses background noise while retaining land features in remote-sensing images.

This study leverages high-resolution optical remote sensing data (from sources like VNREDSat-1, SPOT 5/6/7) sourced from the Vietnam National Remote Sensing Department's Remote Sensing Receiving Station. The goal is to enhance the accuracy of subsidence analysis. By examining these datasets, the study filters out less reliable points, especially those linked to dynamic entities such as water bodies and vegetation, or locations undergoing land use transitions or construction. Two methodologies are employed to exclude low-reliability PS points: (1) Optical satellite imagery is used to identify and discard PS points associated with uncertain targets; (2) multi-temporal optical satellite imagery helps in identifying and eliminating PS points located in areas of land cover change. To pinpoint PS points on aquatic surfaces swiftly, a water mask is generated using the Normalised Difference Water Index (NDWI), drawing from the NIR and Green bands of SPOT6/7 imagery. GIS tools are then employed to select and excise all PS points located on these water surfaces.

Subsidence mapping and database establishment

The derivation of subsidence contour lines from the selected PS points is accomplished through an automated interpolation technique referred to as Spatial Analysis. This technique employs a square grid with a grid spacing of 2 km. The subsidence values of PS points within each grid cell are aggregated to compute the subsidence value for that specific cell (corresponding to a single pixel). These pixel-level values undergo a secondary interpolation process to generate subsidence isolines with intervals of 10 mm. These isolines are then categorised into four distinct zones: the non-subsidence zone (with a subsidence value of 0 mm), zones with subsidence risk up to 5 cm, zones with subsidence values ranging between 5 cm and 10 cm, and zones with subsidence values surpassing 10 cm. The systematic division of these subsidence zones aligns with the classification standards established by the Vietnam Department of Survey, Mapping and Geographic Information (DOSM).

Outcomes yielded by various subsidence zoning methodologies are standardised to facilitate comprehensive analysis and seamless integration in the study. In this zoning classification, distinguishing between low, medium, and high subsidence levels, the subsidence isolines featured on the map provide intricate insights into regions marked by increments of 1 cm of subsidence.

In the final stages, data would be standardised and mapped based on the guidelines of MONRE (2011), and the database would be established based on the guidelines of MONRE (2014) [31,32].

Reliability assessment of subsidence monitoring results

Based on the results of (1) surface subsidence monitoring in Ho Chi Minh City using PSI technique based on Sentinel-1 from 2017 to 2019 [14] and (2) field survey results of land subsidence monitoring using Automatic Level in Ho Chi Minh City from 2014 to 2020 [13] a comparison was made between subsidence trends and monitoring methods at the same time intervals. This allowed for a holistic comparison, validation, and assessment of ground subsidence trends in Ho Chi Minh City, which used various land subsidence monitoring techniques.

Results

Land subsidence in Ho Chi Minh City

Figure 2 shows the subsidence level in Ho Chi Minh City, which is divided into four categories: non-subsidence areas, areas at risk of subsidence up to 5 cm, areas with subsidence values between 5 cm to 10 cm, and areas with subsidence values exceeding 10 cm. This division aligns with the regulations set forth by DOSM for land subsidence zoning.

In this context, the iso-settlement line is divided into elevation intervals according to the settlement level in millimetres by shifting the radar beam's field of view vertically in the direction of the ground displacement. The value (−) indicates land surface subsidence, and the value (+) indicates land surface rising.

Land subsidence results in Ho Chi Minh City from 2014 to 2021 show that 98,278 km^2 had subsided by over 10 cm, 214,593 km^2 had subsided by 5 to 10 cm, and 1.377,897 km^2 had subsided by less than 5 cm (Figure 2). The land subsidence centre of over 10 cm consists of a part of Binh Chanh district, District 8 (Ward 6, Ward 7, Ward 14, Ward 15, Ward 16), District 6 (Ward 3, Ward 4, Ward 7, Ward 8, Ward 10). Areas with a subsidence level of 5–10 cm in the period of 2014–2021 are in district 6; district 8; Binh Chanh district; Nha Be district; District 4 (Ward 4, Ward 13, Ward 14, Ward 15, Ward 16, Ward 18); district 12 (Thu Thiem ward); Binh Thanh district; the area adjacent to Thinh Loc ward of district 12; Hoc Mon district (Nhi Binh commune); District 9 (some areas in Binh My, Long Phuc ward). The area without subsidence is in Cu Chi district. The remaining areas have subsidence levels of less than 5 cm. Figure 3 shows the subsidence velocity map in Ho Chi Minh City (from 2014 to 2021). The subsidence velocity varied across different locations and speeds, corresponding to the distribution of subsidence areas from 2014 to 2021.

The area of heaviest subsidence is the Mui Tau roundabout, which is located at the border between two districts of Binh Tan and District 6. The trend shows that this area has a stable movement with a total vertical displacement of 40 to 110 mm in 7 years, corresponding to the vertical subsidence velocity from 5 to 16 mm/year (Figure 4).
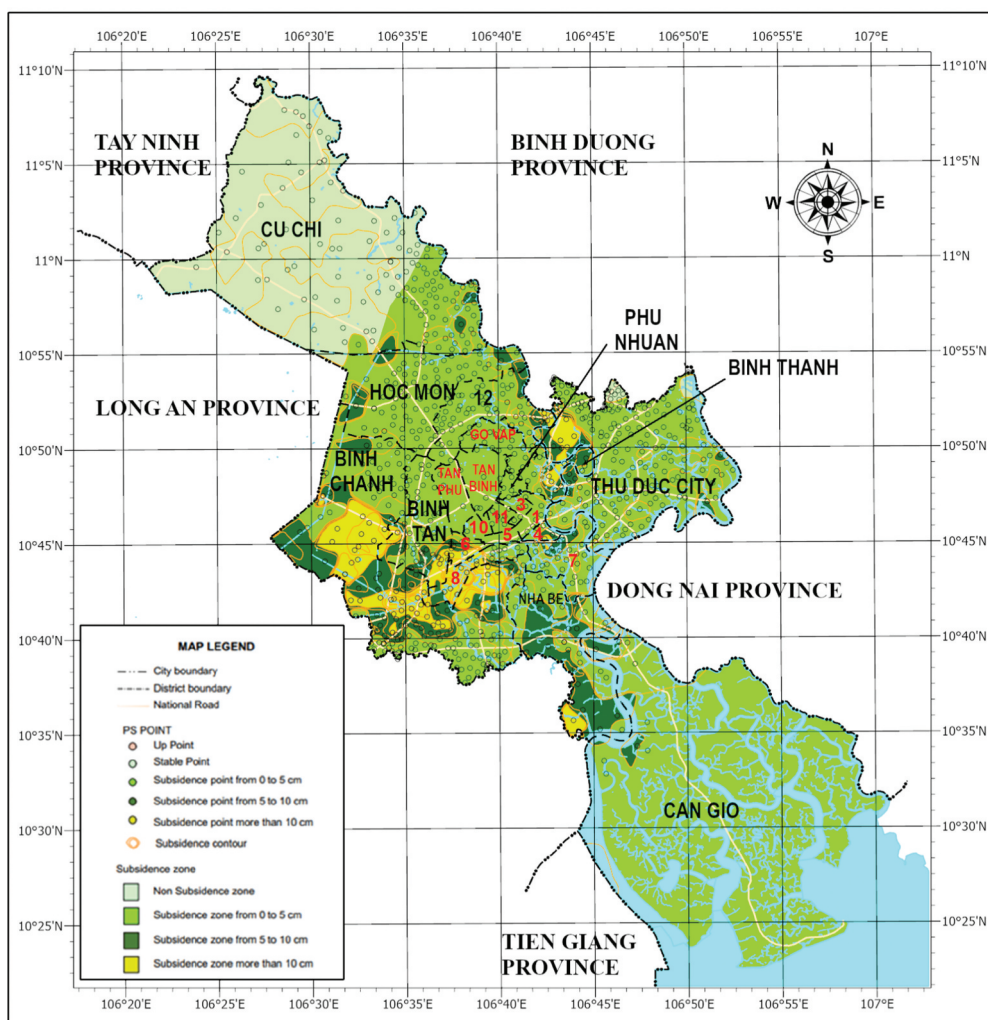
Figure 2. Distribution of land subsidence velocity in Ho Chi Minh City (from 2014 to 2021).

Reliability assessment of subsidence monitoring results

Calculation result on land surface subsidence in Ho Chi Minh City by PSI method was used to compare other results to verify and evaluate the reliability. The results of comparison, verification, and evaluation are as follows:

Duffy et al. [14] used the PSI technique and 121 Sentinel-1 images covering Ho Chi Minh city in the period from 2017 to 2019. This study showed how openly available Sentinel-1 data can be used to retrieve precise and up-to-date vertical displacements for the metropolitan area of Ho Chi Minh City. Results show that the observed average subsidence rates were 3,3 mm per year with a maximum local subsidence of 5,3 cm per year. The study indicated the need for similar localised analysis in dynamic, rapidly urbanising coastal areas subject to heterogeneous deformation and provided details on
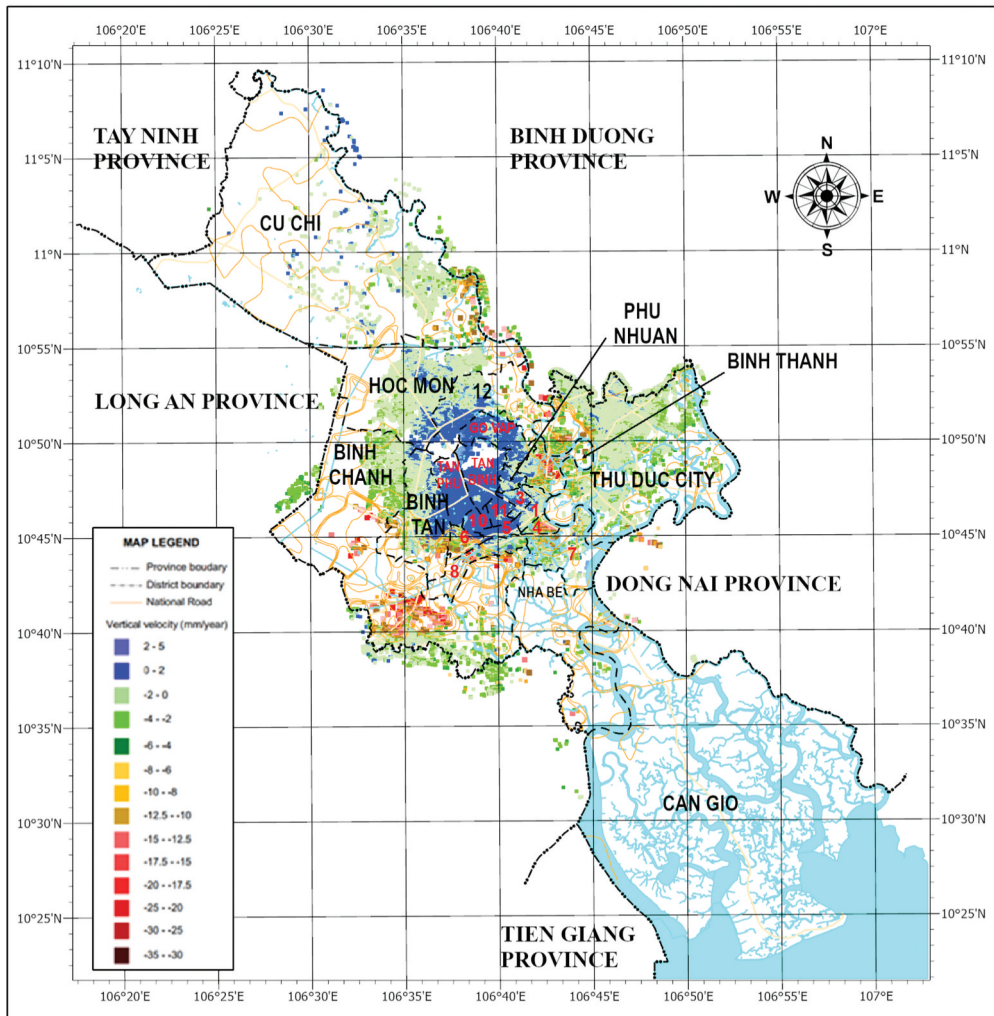
Figure 3. Subsidence velocity map in Ho Chi Minh City (from 2014 to 2021).

the application of PSI processing with freely available Sentinel-1 data for continuous assessment.

In comparing subsidence rate trends between the publication of Duffy et al. [14] and the present research, the result shows that there is a similarity in subsidence area and trend (Figure 5(a,b)). But, subsidence velocity is different because the monitoring period of the current study is longer (2014–2021) compared to the publication (2017–2019).

On the other hand, the field survey results of land subsidence monitoring use Automatic Level with annual frequency in Ho Chi Minh City in the same period of 2014–2020. The number of highly reliable points for land subsidence comparison is 6 (Table 1).

Since two data sources yield results from two different methods, there are different properties: PS points are collected from images at the beginning and end of the year, but field survey points are collected from June to the end of the year. These points do not
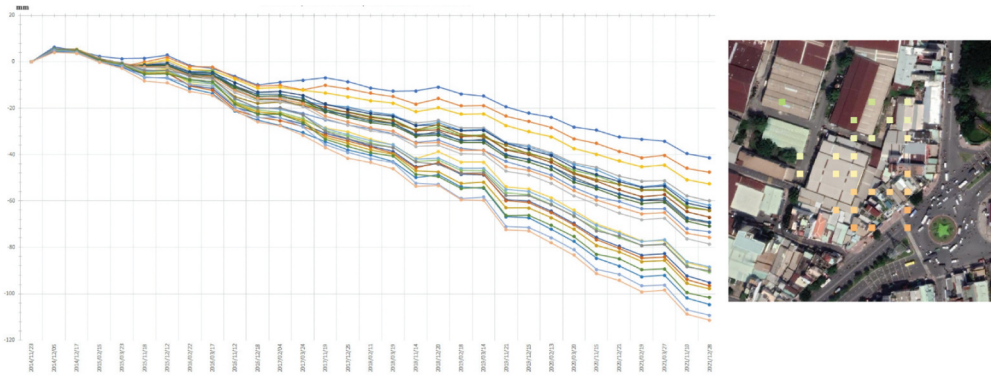
Figure 4. The trend of the vertical displacement at PS points at Mui Tau roundabout.

Subsidence zone

- Non Subsidence zone
- Subsidence zone from 0 to 5 cm
- Subsidence zone from 5 to 10 cm
- Subsidence zone more than 10 cm

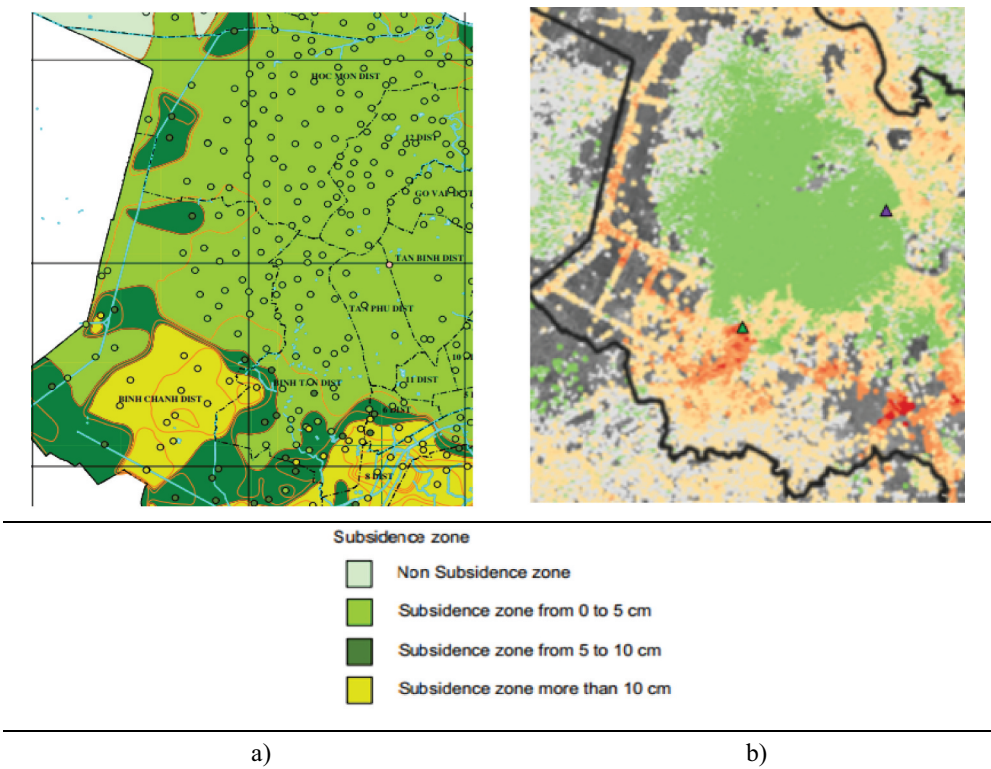a)   b)

Figure 5. a) Extracted portion of subsidence monitoring results for Ho Chi Minh City from the current research phase, spanning from 2014 to 2021. b) Extracted portion of subsidence monitoring results for Ho Chi Minh City from Duffy et al. [14], covering the period from 2017 to 2019.

overlap in exact location. For comparison purposes, it is necessary to expand around the location of the land subsidence monitoring point by a radius of 100 m, then compile statistics of PS points within that range and take the average value of points for comparison and verification. The table below shows the comparison results of land subsidence.

Table 1. The summary of comparison between the levelling results and PSI results.

STT	Name of Mark	Velocity (mm/year)		Deviation (mm)
		Levelling	PS-INSAR	
1	I(VL-HT)256	−18,0	−15,7	2,3
2	I(VL-HT)265	−1,1	−2,8	−1,7
3	II(GD-APĐ)8	1,9	−0,22	−2,1
4	II(TX-TL)5	−3,6	−2,06	1,5
5	II(TX-TL)6	−3,4	−2,3	1,1
6	III(HM-LMX)1	1,6	−2,2	−3,8

Comparison results also show similarities in land subsidence trends for the two methods. Nevertheless, different methods, influenced by various factors in calculation process, will produce different absolute subsidence values.

Discussions

Land subsidence can be caused by a variety of processes. Dinh et al. [13] and Hooper et al. [33] mentioned that there are two drivers for the subsidence phenomena, namely: (1) natural processes, in which the geological signature plays an important role; and (2) mixed processes, which, because of urbanisation, exacerbate the subsidence problem.

Persistent Scatterer Interferometry (PSI) techniques were used to assess the evolution of subsidence using radar data series. Persistent Scatterer Interferometry tracks changes over time by using the phase history of scatterers with a strong amplitude, referred to as Persistence Scatterers (PS points). The PSI technique and openly available Sentinel-1 data can be used to retrieve precise and up-to-date vertical displacements for the metropolitan area of Ho Chi Minh City [12,34,35].

Results of Sentinel-1A imagery processing using PSI technology show the distribution and area of uneven land subsidence in Ho Chi Minh City in the period from 2014 to 2021. The subsidence area over 10 cm is about 98.278 km^2, from 5 to 10 cm is about 214.593 km^2, and less than 5 cm is about 1377.897 km^2. The result in the period 2005–2014 of Ho Chi Minh City, investigated by Vietnam Department of Survey, shows that the land subsidence centres of over 10 cm were in District 11, District 5 and a small part of Binh Chanh district (Binh Hung, Phong Phu, An Phu Tay, Tan Tuc, Ton Kien communes) [35]. Compared to this study results, the land subsidence centre of over 10 cm has changed to another part of Binh Chanh district, District 8 (Ward 6, Ward 7, Ward 14, Ward 15, Ward 16), District 6 (Ward 3, Ward 4, Ward 7, Ward 8, Ward 10). Three new areas with subsidence of over 10 cm appeared. The first region was in Le Minh Xuan commune, bordering Tan Tao, Binh Loi, Tan Nhut wards of Binh Chanh district; the second region in wards 25, 26, 27 of Binh Thanh district, Hiep Binh Chanh ward, Hiep Binh Phuoc ward of Thu Duc City, a part of An Phu Dong ward of District 12; the third region in Hiep Phuoc ward, Nha Be district.

Areas with a subsidence level of 5–10 cm in the period of 2014–2021 are in district 6; district 8; Binh Chanh district; Nha Be district; Ward 4, Ward 13, Ward 14, Ward 15, Ward 16, Ward 18 of District 4; Thu Thiem ward of district 12; Binh Thanh District; the area adjacent to Thinh Loc ward of district 12; Nhi Binh commune of Hoc Mon district; some areas in Binh My, Long Phuc of District 9. The area without subsidence is in Cu Chi district. The remaining areas have subsidence levels of less than 5 cm. Figure 3 shows the subsidence velocity map in Ho Chi Minh City (from 2014 to 2021). The subsidence

velocity varied across different locations and speeds, corresponding to the distribution of subsidence areas from 2014 to 2021.

Especially affected is the Mui Tau roundabout, which is located at the border between Binh Tan District. This area has the heaviest subsidence. The trend shows that this area has a stable movement with a total vertical displacement of 40 to 110 mm in 7 years, corresponding to a vertical subsidence velocity from 5 to 16 mm/year.

Chen et al. [11] confirmed that the integration of the InSAR time series method with IBI index to analyse the relationship between urbanisation and land subsidence is highly beneficial. Additional factors such as building styles, weights, and plot ratios are necessary for a more comprehensive analysis and better assessment of the influence of urbanisation on land subsidence. In this study, using the ArcGIS tool and optical satellite imagery data helped remove PS points from uncertainty targets in areas of land cover change. Such targets include water surfaces (ponds, lakes, water channels, rivers, etc.) and plant surfaces, as well as trees in parks and urban areas. Over seven years, the tree's structure can undergo significant changes because of growth, external environmental impact, and urban maintenance and landscaping activities. All PS points within a tree canopy will be removed. For example, the coherence of the PS point in Figure 6 is 0,53 but this point within the plant canopy is found and removed. To select the PS points on the water surface quickly, a water mask will be created using the Normalised Difference Water Index (NDVI) derived from NIR and Green bands of high-resolution optical remote sensing data. This process will select identify and remove all uncertain PS points in areas of land cover change. Owing to infrastructure construction and urban development, Ho Chi Minh City's land cover and land use changed rapidly from 2014 to 2021. Multi-temporal optical satellite image data from 2014–2021, along with reference data from Google, were used to detect and remove PS points in these changing areas.

Moreover, the discussion in the section 'Reliability assessment' compares our results with field survey data obtained using a digital-level machine during the same research period. The discussion in the 'Reliability assessment' section compares our results to field
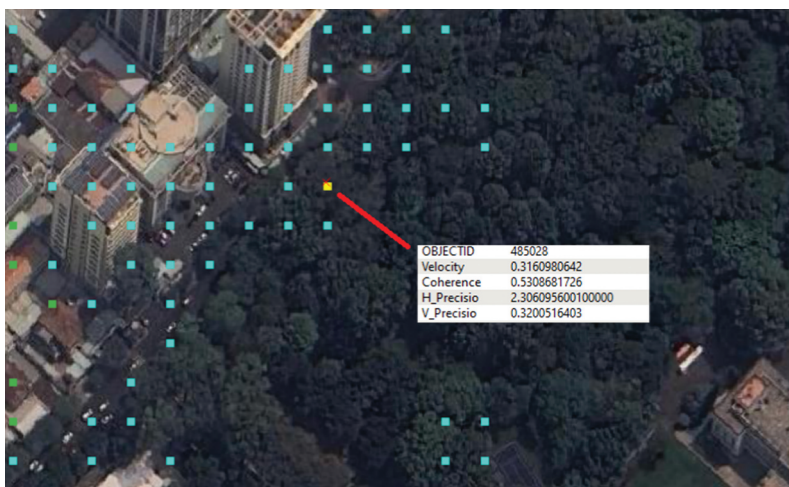

Figure 6. The illustration of PS point filtering.

survey data obtained using a digital-level machine during the same research period. Comparing our findings with previously published research will further validate the accuracy of the results obtained from Sentinel-1A imagery processing using the PSI technique.

Conclusions

The PSI technique applied to Sentinel-1A imagery for land surface subsidence research is gaining widespread acceptance globally. The results from monitoring subsidence movements using differential interference technology in Ho Chi Minh City from 2014 to 2021 are reliable. Zoning based on radar differential interference has effectively revealed areas of land surface movement at varying levels, especially in expansive regions like Ho Chi Minh City. These findings are in close agreement with on-ground subsidence monitoring datasets. Additionally, when these results are compared with PS points processed by differential interferometry using other radar images from both international and domestic sources, the subsidence rates across different areas of the project site appear consistent. Beyond giving a broad general view of subsidence velocities, the data also offer a granular analysis of localised subsidence rates, indicating whether the trends in specific areas are stable, increasing, or decreasing. These trends often correlate with both natural and man-made changes on the land surface. To enhance the accuracy of subsidence monitoring, it is crucial to employ filtering methods using multi-temporal optical images. Validating these results by comparing them with field survey data, obtained using a digital level machine during the same research period, and referencing other published studies can bolster the reliability of our findings.

References

[1] MONRE, 2022, *Report Overall Project to Investigate and Evaluate for Underground Water Exploitation and Use, and its Impact on Land Surface Subsidence in Hanoi City, Ho Chi Minh City, and Mekong Delta; Orientation in Management, Exploitation and Sustainable use of Underground Water Resources* (Hanoi: Ministry of Natural Resources and Environment of Vietnam).

[2] Aditiya, A., Takeuchi, W. and Aoki, Y., 2017, Land subsidence monitoring by InSAR time series technique derived from ALOS-2 PALSAR-2 over Surabaya City, Indonesia. *The 5th Geoinformation Science Symposium (GSS 2017) IOP Conference Series: Earth and Environmental Science* **98**, 012010. doi: 10.1088/1755-1315/98/1/012010

[3] Sandwell, D.T. and Price, E.J., 1998, Phase gradient approach to stacking interferograms. *Journal of Geophysical Research Atmospheres* **103**(B12), 30183–30204. doi: 10.1029/1998JB900008

[4] Ferretti, A., Prati, C. and Rocca, F., 2000, Nonlinear subsidence rate estimation using permanent scatterers in differential SAR interferometry. *IEEE Transactions on Geoscience and Remote Sensing* **38**(5), 2202–2212. doi: 10.1109/36.868878

[5] Ferretti, A., Prati, C. and Rocca, F., 2001, Permanent scatterers in SAR interferometry. *IEEE Transactions on Geoscience and Remote Sensing* **39**(1), 8–20. doi: 10.1109/36.898661

[6] Boni, R., Meisina, C., Perotti, C. and Fenaroli, F., 2015, PSI-based methodology to land subsidence mechanism recognition. *Conference Proceedings, International Association of Hydrological Sciences* **372**, 357–360. doi: 10.5194/piahs-372-357-2015

[7] .Cuong, T.Q., Dinh, H.T.M., Trung, L.V. and Thuy, L.T., 2015, Ground subsidence monitoring in Vietnam by multi-temporal InSAR technique. Conference: IGARSS 2015 – 2015. *IEEE International Geoscience and Remote Sensing Symposium*. doi: 10.1109/IGARSS.2015.7326585.

[8] Rosi, A., Tofani, V., Agostini, A., Tanteri, L., Stefanell, C.T., Catani, F. and Casagli, N., 2016, Subsidence mapping at regional scale using Persistent Scatters Interferometry (PSI): The case of Tuscany region (Italy). *International Journal of Applied Earth Observation and Geoinformation* **52**, 328–337. doi: 10.1016/j.jag.2016.07.003

[9] Holley, R., Burren, R. and Abidin, H.Z., 2012, Subsidence mapping in Jakarta - PSI processing of L-band ALOS PALSAR data. Conference proceedings, 'Fringe 2011 Workshop', Frascati, Italy, 19–23 (ESA SP-697, 2012). https://www.researchgate.net/publication/269276115

[10] Mouratidis, A. and Costantini, F., 2012, PS and SBAS interferometry over the broader area of Thessaloniki, Greece, using the 20-year archive of ERS and ENVISAT data. Conference proceedings of 'Fringe 2011 Workshop', Frascati, Italy. https://www.researchgate.net/publication/280025648 .

[11] Chen, B., Gong, H., Li, X., Lei, K., Ke, Y., Duan, G. and Zhou, C., 2015, Spatial correlation between land subsidence and urbanization in Beijing, China. *Natural Hazards* **75**(3), 2637–2652. doi: 10.1007/s11069-014-1451-6

[12] Crosetto, M., Devanthéry, N., Cuevas-González, M., Monserrat, O. and Crippa, B., 2015, Exploitation of the full potential of PSI data for subsidence monitoring. *Conference Proceedings, International Association of Hydrological Sciences* **372**, 311–314. doi: 10.5194/piahs-372-311-2015

[13] Dinh, H.T.M., Trung, L.V. and Thuy, L.T., 2015, Mapping ground subsidence phenomena in Ho Chi Minh City through the radar interferometry technique using ALOS PALSAR data. *Remote Sensing* **7** (7), 8543–8562. 10.3390/rs70708543

[14] Duffy, C.E., Braun, A. and Hochschil, V., 2020, Surface subsidence in urbanized coastal areas: PSI methods based on sentinel-1 for Ho Chi Minh City. *Remote Sensing* **12**(24), 4130. doi: 10.3390/rs12244130

[15] Vicari, A., Famigliettia, N.A., Colangelo, G. and Cecere, G., 2019, A comparison of multi temporal interferometry techniques for landslide susceptibility assessment in urban area: An example on stigliano (MT), a town of Southern of Italy. *Geomatics, Natural Hazards and Risk* **10**(1), 836–852. doi: 10.1080/19475705.2018.1549113

[16] Cigna, F., Ramírez, R.E. and Tapete, D., 2021, Accuracy of sentinel-1 PSI and SBAS InSAR displacement velocities against GNSS and geodetic leveling monitoring data. *Remote Sensing* **13**(23), 4800. doi: 10.3390/rs13234800

[17] Holzer, T.L. and Johnson, A.I., 1985, Land subsidence caused by groundwater withdrawal in urban areas. *Geo Journal* **11**(3), 245–255. doi: 10.1007/BF00186338

[18] Ha, T.H., Luyen, B.K., Hung, Q.H. and Huong, K.T.T., 2023, Christoph Butscher. Proposal of study on InSAR-based land subsidence analysis as basis for subsequent hydro-mechanical modeling: A case study of Hanoi, Vietnam. Conference proceedings of "Advances in Geospatial Technology in Mining and Earth Sciences", Hanoi, Vietnam, 535–548.

[19] Richa, B., Haireti, A., Aikebaier, M. and Akihiko, K., 2017, Detection of land subsidence in Kathmandu Valley, Nepal, using DInSAR technique. *Land* **6**(2), 39. doi: 10.3390/land6020039

[20] Nguyen, Q.T., 2016, The main causes of land subsidence in Ho Chi Minh City. *Procedia Engineering* **142**, 333–340. doi: 10.1016/j.proeng.2016.02.058

[21] Anh, T.V. , 2021, Temporal sentinel-1 radar images. 4th asia pacific meeting on near surface. *Geoscience & Engineering*, 2021. doi: 10.3997/2214-4609.202177035.

[22] Anh, T.V., Nam, B.X., Long, N.Q. and Anh, T.T., 2020, Land subsidence detection in Tan My-Thuong Tan Open pit mine and surrounding areas by time series of sentinel-1 images. *Inżynieria Mineralna* **1**(2), 171–180. doi: 10.29227/IM-2020-02-22

[23] Anh, T.V., Cuong, T.Q., Anh, N.D., Dinh, H.T.M., Anh, H.T., Khien, H.T. and Dieu, B.T., 2020, Subsidence assessment of building blocks in Hanoi Urban Area from 2011 to 2014 using TerraSAR-X and COSMO-SkyMed images and PSInSAR. *Conference Proceedings, Remote Sensing and GIScience* 127–150. doi: 10.1007/978-3-030-55092-9_8

[24] Nam, B.X., Anh, T.V., Luyen, B.K., Long, N.Q., Ha, L.T.T. and Goyal, R., 2020, Mining-induced land subsidence detection by persistent scatterer in SAR and sentinel-1: Application to Phugiao Quarries, Vietnam. *Proceedings of the International Conference on Innovations for Sustainable and Responsible Mining* 18–38. doi: 10.1007/978-3-030-60269-72

[25] Galloway, D.L. and Hoffmann, J., 2007, The application of satellite differential SAR interferometry-derived ground displacements in hydrogeology. *Hydrogeology Journal* **15**(1), 133–154. doi: 10.1007/s10040-006-0121-5

[26] Hoffmann, J., Zebker, H.A., Galloway, D.L. and Amelung, F., 2001, Seasonal subsidence and rebound in Las Vegas Valley, Nevada, observed by synthetic aperture radar interferometry. *Water Resources Research Journal* **37**(6), 1551–1566. doi: 10.1029/2000WR900404

[27] Jalilibal, Z., Amiri, A., Castagliola, P. and Khoo, M.B.C., 2021, Monitoring the coefficient of variation: A literature review. *Computers & Industrial Engineering Journal* **161**, 107600. doi: 10.1016/j.cie.2021.107600

[28] Gaber, A., Darwish, N. and Koch, M., 2017, Minimizing the residual topography effect on interferograms to improve DInSAR results: estimating land subsidence in Port-Said City, Egypt. *Remote Sensing* **9**(7), 752. doi: 10.3390/rs9070752

[29] Xu, H., 2008, A new index for delineating built-up land features in satellite imagery. *International Journal of Remote Sensing* **29**(14), 4269–4276. doi: 10.1080/01431160802039957

[30] Shang, Y., 2000, On extraction and fractal of urban and rural residential spatial pattern in developed area. *Acta Geographica Sinica* **55**(6), 671–678. doi: 10.11821/xb200006004

[31] MONRE, 2011, *Circular No. 37/2011/TT-BTNMT on Economic - Technical Norms for Thematic Mapping Establishment at the Scale of 1:25,000, 1:50,000, 1:100,000, 1:250,000 Using Satellite Image Data* (Hanoi: Ministry of Natural Resources and Environment of Vietnam).

[32] MONRE, 2014, *Circular No. 26/2014/TT-BTNMT Promulgating the Process and Economic-Technical Norms for Database Building of Natural Resources and Environment* (Hanoi: Ministry of Natural Resources and Environment of Vietnam).

[33] Hooper, A., Segall, P. and Zebker, H., 2007, Persistent scatterer interferometric synthetic aperture radar for crustal deformation analysis, with application to Volcán Alcedo, Galápagos. *Journal of Geophysical Research: Atmospheres* **112**(B7). doi: 10.1029/2006JB004763.

[34] Ngoc, T.D.T., Perset, M., Strady, E., Phan, T.S.H., Vachaud, G., Quertamp, F. and Gratiot, N., 2016, Ho Chi Minh City. Growing with water-related challenges. In: A. Aureli, D. Jean-Claude, I. Géraldine, J.C. Blanca, L. Cléo, M. Ismael, M. Alexandros, N. Bruno, S. Irina, T. Jean-Pierre and T. Bruno (Eds) *Water, Megacities and Global Change* (Paris: UNESCO/ARCEAU), pp. 46–49. https://www.researchgate.net/publication/310464909

[35] Vietnam Department of Survey, 2022, Mapping and geographic information (DOSM). Report on "Surveying result of state elevation milestones system results at the level of I, II, III in Ho Chi Minh City and the Mekong Delta - Local subsidence monitoring", Hanoi, Vietnam. (Hanoi, Ministry of Natural Resources and Environment of Vietnam).